PICOSECOND TRANSIENT ABSORPTION SPECTRA AND THE TWISTED INTRAMOLECULAR CHARGE TRANSFER PHENOMENON

J. Dobkowski, Z.R. Grabowski*, J. Jasny and Z. Zieliński

Institute of Physical Chemistry, Polish Academy of Sciences
Kasprzaka 44, 01-224 Warszawa, Poland

*Dedicated to Professors Zdzisław Ruziewicz and Krzysztof Pigoń
on the occasion of their 70th birthdays[†]*

An improved model of a computer-controlled picosecond absorption spectrometer was designed and constructed. Its operation is described, and applied to the measurement of transient spectra of p-N, N-dioctylamino--acetophenone. The spectroscopy and photophysics of this compound are compared to the other compounds exhibiting the dual fluorescence, assigned usually to the adiabatic formation of the "twisted" intramolecular charge transfer excited state. The data are discussed in relation to alternative suggestion of an inversion of the pyramidal amino nitrogen atom. The whole evidence supports the decoupling of the π-electronic systems of D^+ and A^- in the D^+–A^- polar excited state, in full accord with the "twisted" intramolecular charge transfer model. The peculiar behaviour of the long alkyl $-NR_2$ derivatives (favouring the "twisted" intramolecular charge transfer state emission) seems to be primarily due to the decreasing oxidation potential of such electron donor groups.

PACS numbers: 36.20.Kd, 06.60.In

1. Introduction

Numerous molecules built of an electron donor (D) and electron acceptor (A) linked together by the single bond (i.e., D–A molecules) exhibit a peculiar behaviour in their low-laying electronically excited states. A polar solvent assisted, very fast but thermally activated adiabatic reaction occurs, leading to a highly polar excited state. In favourable cases (if there is in the ground state a considerable barrier to internal rotation) two fluorescence bands appear, the primary

---

*and the College of Science in Warsaw.
[†]Submitted on invitation of the Institute of Physical and Theoretical Chemistry, Technical University of Wrocław, Wrocław, Poland.

emission described as F_b, the secondary (from the polar emitting state) — F_a. The nature of the polar emitting state, since the discovery of the dual fluorescence of p-N,N-dimethylamino-benzonitrile (DMABN) by Lippert et al. [1] had been the subject of numerous controversial hypotheses. Now, the most generally accepted hypothesis [2] is the one of the "twisted" intramolecular charge transfer state (TICT) according to which the D and A moieties, limited in their structural degrees of flexibility, twist to orthogonality of their π-electronic systems [3, 4]. Among the recently supported principally opposing hypotheses there are those assigning the dual fluorescence of DMABN and structurally related compounds either to the formation of exciplexes with the solvent [5], or to the pseudo Jahn–Teller distortion [6, 7]. Marginally: both these views mutually oppose.
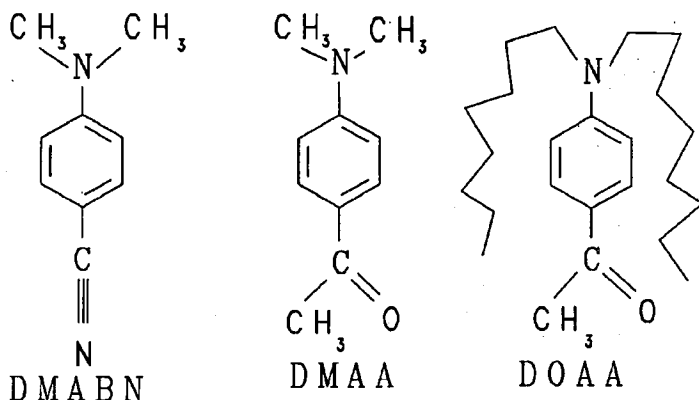
Cognition of the molecular structure of an excited singlet state is most frequently done by one of the following ways: (i) quantum chemical calculation at different levels of sophistication; (ii) comparison of the electronic absorption (from the ground state, $S_n \leftarrow S_0$) and fluorescence spectra ($S_1 \rightarrow S_0$) (Franck–Condon analysis; Stokes' shift; solvatochromic shifts; polarization; factors affecting the kinetics); (iii) assignment of the transient absorption spectrum from the excited state, $S_n \leftarrow S_1$.

Quantum chemical calculations, starting from early papers [3] to the recent highly advanced quantum-chemical description of the DMABN molecule by Roos et al. [8], support the existence of a highly polar state ($\mu \approx 15$–19 D) as one of the lowest excited states in the free molecule in its twisted (orthogonal) conformation; stabilization by polar solvents turns this state to the lowest excited singlet state (inaccessible directly in absorption, due to the Franck–Condon rule). Such result has been obtained also for p-dimethylamino-benzaldehyde (DMABA), a carbonyl derivative closely related to, and of the same π-electronic structure as, DMAA and DOAA [9].

Luminescence was the main evidence in large majority of the relevant papers. For DMAA the evidence is first delivered by the comparative study of the model compounds [10].

Transient absorption spectra, in a few cases reported until now, give the real key to understand the electronic structure of the F_a emitter. For DMABN [11] and DMAA [12] the transient absorption spectra in the visible were matching the spectra of the corresponding radical anion, A^-: that of benzonitrile$^-$ or acetophenone$^-$, respectively [13].

Considering the transient absorption spectra the most important evidence in disclosing the nature of the discussed polar state, we decided to build the picosecond absorption spectrometer. The inspiration was borrowed initially from the apparatus built in Bordeaux by Rullière and his students [14], then modified and completed in many respects.

Zachariasse et al. [6] reported that the dialkylamino-benzonitriles with the methyl groups replaced by longer alkyls emit the long-wave F_a band with much higher relative yield than DMABN. For the internal rotation one could expect the contrary: large, voluminous groups should slow down the internal rotation. The effect of the large dialkylamino-groups awaited an explanation.

The subject of this paper is a comparison of the spectra and photophysics of DMAA and DOAA, specially of the transient absorption spectra, to elucidate the nature of the highly polar (TICT ?) states. The measurements of the transient absorption were carried out with the just built original picosecond absorption spectrometer.

2. Experimental

2.1. Compounds and synthesis

Synthesis of 4-N, N-dioctylamino-acetophenone (DOAA): 4-amino acetophenone was boiled for 12 hours in n-octanol with fourfold excess of n-octyl iodide, fivefold molar quantity of anhydrous K_2CO_3 and a catalytic quantity of KI. Excess of octyl iodide and octanol was removed by distillation with water vapour, the cooled residual extracted with ether, dried, and after removal of ether dissolved in hexane. After filtering off some crystalline 4-octylamino-acetophenone, the solution was evaporated and the residual distilled. Pale yellowish liquid, b.p.: 278°C ($p = 10$ mm Hg); ^{1}H NMR (CDCl$_3$) supported the structure.

DMAA was purified as described earlier [9]. Ether, tetrahydrofuran (THF) and acetonitrile (ACN) were of spectroscopic purity (MERCK).

2.2. Stationary fluorescence measurements

Stationary fluorescence spectra were measured with Jasny spectrofluorimeter [15], much modified and equipped with a photon counting detection system. The spectra are corrected for the instrumental response.

3. Picosecond spectrometer

3.1. Construction and operation

The computer-controlled picosecond spectrometer (Fig. 1) is based on the passively mode-locked Nd:YAG laser system (EKSPLA, Lithuania) as the light source. The negative feedback control system stabilizes the mean pulse energy. A single pulse ($\tau \approx 25$ ps fwhm, $\lambda = 1064$ nm) is selected by an opto-electronic
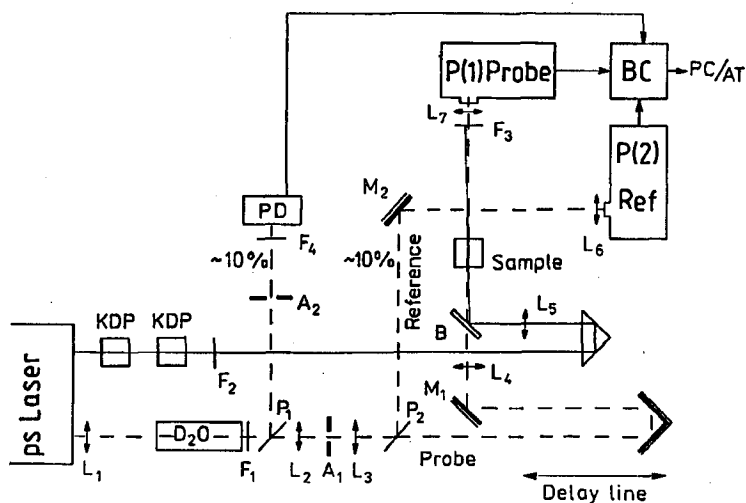
Fig. 1.   Optical scheme of the picosecond spectrometer for transient absorption measurements. L_1 — lens, $f = 650$ mm; F_1, F_2 — optical edge filters (cut-off 1064 nm); P_1, P_2 — quartz plates; L_2, L_3 — achromatic lens, $f = 85$ mm; A_1 — aperture 0.2–0.6 mm; M_1, M_2 — mirrors; L_4 — achromatic lens, $f = 192$ mm; L_5 — lens, $f = 200$ mm; B — dielectric mirror (chromatic beam splitter) reflective in UV, transparent in the visible; F_3 — optical filter (cut-off UV); L_6, L_7 — achromatic collective lens, $f = 35$ mm; P(1), P(2) — polychromators with photodiode array detectors; BC — buffer memory and contol unit; A_2 — controlled aperture; F_4 — interference filter, $\lambda_{max} = 600$ nm; PD — photodiode.

pulse selector, amplified, and split in two beams (pulse energy about 20 mJ each). The first beam is directed into the KDP crystals to generate higher harmonic frequencies. Third harmonic, $\lambda = 355$ nm, is used as the excitation beam.

The other beam of the fundamental frequency is focused inside the long cell with D_2O to generate the pulse of spectral continuum extending between 430 and 800 nm (cf. Fig. 3A, curve a), used as the probe. As any large variation of the pulse intensity can affect the spectral distribution of the continuum [16], the intensity of the latter is controlled by a photodiode (PD) at the fixed $\lambda = 600$ nm.

The spectral distribution is monitored by splitting the continuum in two, the reference and the probe beam, each focused into the slit of the corresponding polychromator, P(2) or P(1), respectively. Each Jasny model polychromator contains the concave holographic grating (JOBIN-YVON) with a flat focusing field where the photodiode array (RETICON RL 1024 S) is situated. Relative aperture $f/3.2$, spectral resolution ≈ 0.4 nm/diode.

The analog signals from the diode arrays are digitized and transmitted to the buffer memory, and next to the PC. The probe pulses are delayed in the specially designed variable optical delay line with the roof mirrors (active area $\phi = 18$ mm each). The length of the optical path in the loop (maximum delay 3.4 ns, single step $\Delta t = 0.1$ ps) can be set manually or preset with a computer-controlled step motor.

Both, probe and excitation beam, cross nearly collinearly the sample (Fig. 1). Finally the probe beam is focused in the slit of the probe polychromator P(1), spectrally resolved and detected by the photodiode array, as in the case of the reference channel.

During the experiments with multiple excitation laser pulses, there is a danger of accumulation of any stable photoproduct in the optical path in the sample, specially in viscous or rigid media. Therefore, a mechanical device is constructed which, before every new excitation pulse, moves the sample in the plane perpendicular to the optical path in such way that the focus of the laser beam draws a Lissajoux curve, and each excitation pulse irradiates a new, intact part of the sample volume [17].

3.2. Measurement procedure

First, the intensities of 50 pulses of the picosecond continuum are measured by the PD photodiode, and their mean $(\bar{I})$ and standard deviation (σ) are statistically evaluated by the computer program. Only the laser shots resulting in continuum intensities within the range $\bar{I} \pm \sigma$ are processed (Fig. 2).
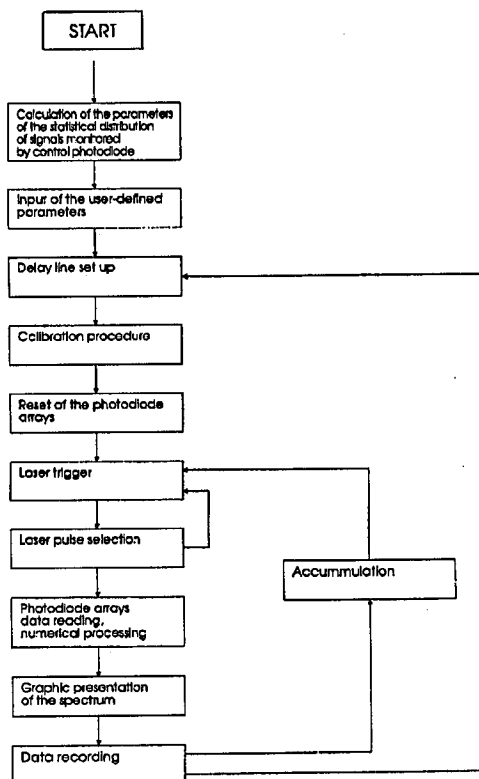

Fig. 2.   Operational scheme of the picosecond spectrometer.

The transient absorption spectrum at a given delay time t_d is calculated from the probe and reference beam signals (S_P and S_R, respectively), with (S) and without (S^0) excitation. The transient absorbance is

$$A(\lambda, t_d) = \log \left[\frac{S_R(\lambda, t_d)}{S_P(\lambda, t_d)} K(\lambda) \right], \tag{1}$$

where the calibration curve

$$K(\lambda) \equiv S_P^0(\lambda) / S_R^0(\lambda). \tag{2}$$

The calibration was carried out for each series of experiments. To improve the S/N ratio, 25–100 spectra are accumulated. The spectra corresponding to Eqs. (1) and (2) are exemplified in Fig. 3.
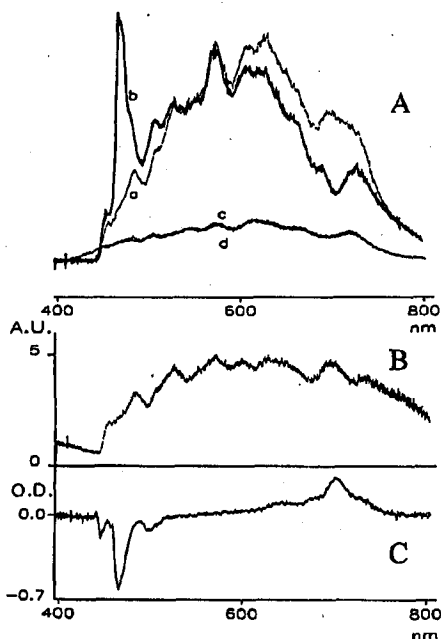

Fig. 3. Transient absorption of pyrene in cyclohexane, delay time $t_d = 100$ ps. Top: ps-continuum as detected by the probe array (P(1) in Fig. 1), a — without, $S_P^0(\lambda)$, and b — with the excitation pulse, $S_P(\lambda)$; c, d — the same detected by the reference array (P(2) in Fig. 1), $S_R^0(\lambda)$ and $S_R(\lambda)$, respectively. Middle part: calibration curve, $K(\lambda)$, as defined in Eq. (2). Bottom: transient spectrum, according to Eq. (1); transient absorption in the long-wave range, peaking around 700 nm, and stimulated emission (negative absorption) between 440 and 513 nm.

4. Results

4.1. Stationary absorption and fluorescence

In liquid solvents DOAA emits two weak fluorescence bands, the "normal" fluorescence F_b, and the "anomalous" fluorescence F_a (Fig. 4). Their quantum
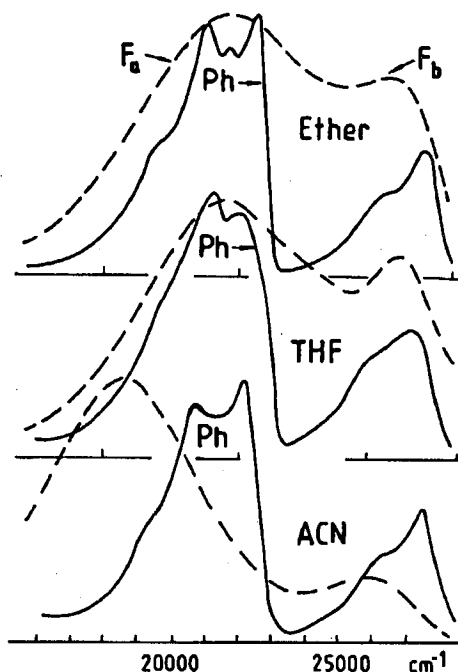
Fig. 4. Luminescence spectra of DOAA in three solvents, excitation 30 000 cm^{-1}: solid curves — $T = 77$ K, fluorescence and phosphorescence (Ph); dashed curves — $T = 293$ K, two fluorescence bands, "normal" F_b, and "anomalous" or "TICT" emission F_a.

TABLE

Comparison of the two fluorescences, F_b and F_a, of DMAA and DOAA, $T = 293$ K: fluorescence maxima (ν_f) and quantum yields (ϕ_f).

Solvent	Band	DMAA		DOAA	
		ν_f [cm^{-1}]	ϕ_f	ν_f [cm^{-1}]	ϕ_f
Ether	F_b	...	...	27 100	4×10^{-4}
	F_a	...	...	21 500	1.3×10^{-3}
THF	F_b	...	...	27 100	4×10^{-4}
	F_a	...	...	21 700	1.3×10^{-3}
ACN	F_b	26 300	0.0018	25 900	0.0025
	F_a	17 900	0.008	18 600	0.016

ϕ_f values of DMAA in ACN: from Ref. [18].

yields strongly depend on the solvent polarity (Table). At 77 K only the F_b fluorescence is observed, along with an intense phosphorescence (Ph) (Fig. 4). In ACN solutions of DOAA the F_a/F_b ratio reaches its maximum at $T \approx 315$ K.

4.2. Fluorescence kinetics

Preliminary experiments demonstrated that the DOAA fluorescence in ACN exhibits a typical bimodal kinetics: the F_b band measured at $\lambda = 360$ nm has a fast decay, $T \leq 20$ ps; F_a, monitored at $\lambda = 580$ nm, has a corresponding rise; both are followed by a slow common decay of the equilibrated system, $B^* \rightleftharpoons A^*$. Such behaviour is very similar to the parent-daughter relation observed in the photophysical kinetics of DMAA [18, 19].

4.3. Transient absorption spectra

Transient absorption spectra of DOAA were recorded in several aprotic solvents of different polarity. Examples are shown in Fig. 5. In weakly polar solvents the absorption maximum is observed at $\lambda \approx 463$ nm. After 2 ns this maximum does not change, whereas the shoulder at $\lambda \approx 500$ nm disappears.
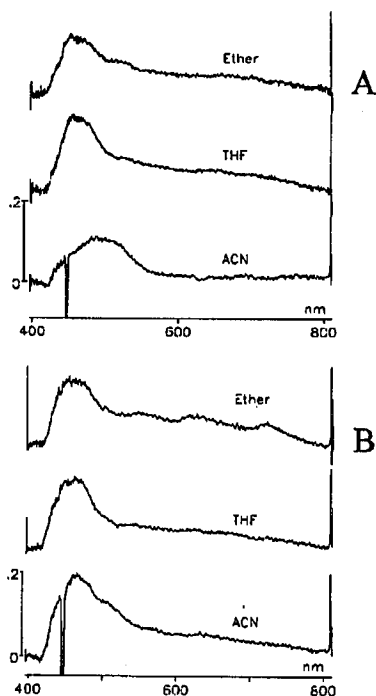

Fig. 5. Transient absorption spectra of DOAA in three solvents of different polarity, $T = 293$ K. A — delay time $t_d = 100$ ps; B — $t_d = 2000$ ps. Optical density scale indicated at the ordinate axis.

In ACN at short t_d the absorption band has a broad maximum at $\lambda \approx 480$–506 nm. At longer t_d the latter absorption decays, giving rise to the band at $\lambda \approx 465$ nm, similar to those in ether or THF. The temporal evolution of the absorption spectrum of DOAA in ACN is shown in Fig. 6.
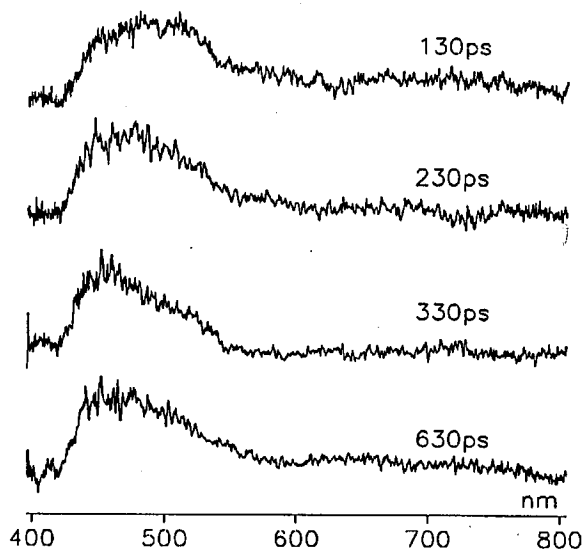
Fig. 6. Temporal evolution of the transient absorption spectrum of DOAA in ACN, $T = 293$ K. Delay time t_d is indicated.

5. Discussion

5.1. Assignment of the transient absorption bands of DOAA

The transient absorption spectra of DOAA (Figs. 5, 6) reveal two distinct features: the short-lived band, decaying along with the rise of the long living (on the time scale of the experiment) band at $\lambda = 465$ nm. The latter is clearly the triplet–triplet absorption, very similar to the $T_n \leftarrow T_1$ absorption of the structurally closely related carbonyl compound, DMABA [20, 21].

The absorption band close to $\lambda \approx 500$ nm resembles very much that of the TICT state of DMAA (identified as characteristic of the species emitting the F_a fluorescence) [12, 13], and is reproducing well the absorption of the radical ion acetophenone$^-$ [22] (Fig. 7)[‡].

Thus, it is to emphasize that the polar emitting state of DOAA is of very similar electronic structure to DMAA, characterized by the absorption localized in the radical anion (A^-) π-electronic subsystem, evidently decoupled from the amino group. The only reasonable model for the decoupling is by the intramolecular $\approx 90°$ rotation: it is a verification of the TICT model.

5.2. Long-chain effects

As to the effect of the long-chain alkyls in the amino group (in fact, the main effect appears between the Me_2N- and Et_2N- substituted compounds), the comparison of photophysics of DMAA and DOAA, as well as of DMABN and its long-chain homologues [6], can be stressed in the following.

[‡] The difference between the spectra of DOAA and DMAA — absence of the triplet absorption in the older spectrum [10] — is due in part to different solvents, but mainly to the loss of sensitivity of the one-time photodiodes in the short-wave range, $\lambda < 470$ nm.
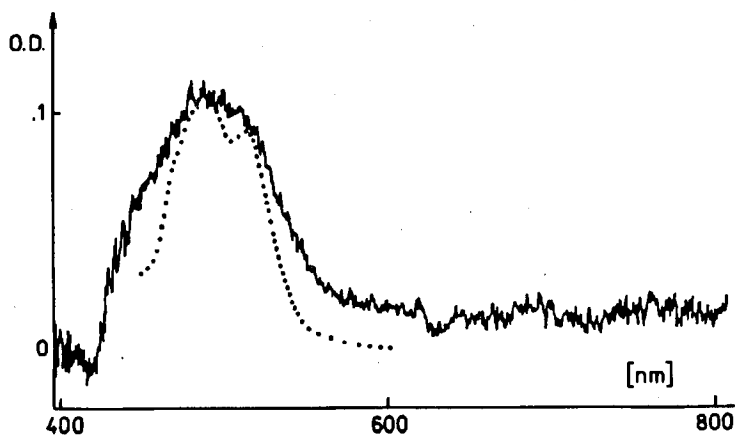
Fig. 7. Transient absorption spectrum of DOAA in ACN, $T = 293$ K, $t_d = 100$ ps. For comparison (dotted curve): the absorption spectrum of radical anion acetophenone⁻ in methyltetrahydrofurane (MTHF), $T = 77$ K [22].

(i) The emission spectra of the compounds with larger alkyl substituents have a markedly higher ϕ_A/ϕ_B ratio than the –NMe$_2$ derivatives, the fluorescence F_a of the homologues of DMABN appearing even in hydrocarbon solvents;

(ii) The F_a transition is shifted with large alkyls to somewhat higher energies than that of the –NMe$_2$ derivatives; this difference is increasing with the polarity of the solvent.

In all studied cases the two emitting states rapidly (as compared to the lifetime) approach the equilibrium, which does not necessarily mean the equilibrium is governing the fluorescence yield. Taking as the limit of reversibility the maximum at the plot $\ln \phi_A/\phi_B$ vs. $1/T$ [23], we find that in ACN the critical temperature $T_1 = 294$ K for DMAA [23], and $T_1 = 315$ K for DOAA; i.e., in each case both, the equilibrium and the kinetics, play a non-negligible role. The radiative rates, k_f, seem not to change with the alkyl size [6].

Contrary to the F_a emission, the F_b band of DOAA is slightly shifted to lower energy as compared to DMAA (Table). To calculate the $h\nu_{max}$ value of the F_a fluorescence of DOAA according to the published model [24], we used as the oxidation potential of trioctylamine that reported for tripentylamine in ACN, $E_{ox} = +0.89$ V vs. SCE [25a], and the Onsager radius ($a_0^3 = 143$ Å^3) resulting from the molecular volume. Assuming the ground state potential barriers and Stokes' shifts in the F_b fluorescence to be the same for DOAA and DMAA, we obtain 19 000 cm^{-1} as the calculated value, in a satisfactory agreement with the observed fluorescence maximum: 18 600 cm^{-1} (Fig. 8).

Thus, it seems that the effect of large alkyl groups, increasing the intensity ratio of two fluorescence bands, F_a/F_b, is mainly due to the lowering of the oxidation potential, i.e. increasing the donor ability, of the dialkylamino group.[§]

[§]There are, however, substantial differences between the reported oxidation potentials of trialkylamines in ACN: NMe$_3$ +1.04 V [25b]; NEt$_3$ +1.15 V [25c]; NProp$_3$ +0.88; +0.91; +0.93 V [25d]; +1.14 V [25f]; NBu$_3$ +0.78 V [25e]; NPent$_3$ +0.89 V [25a]. All values are given here vs.
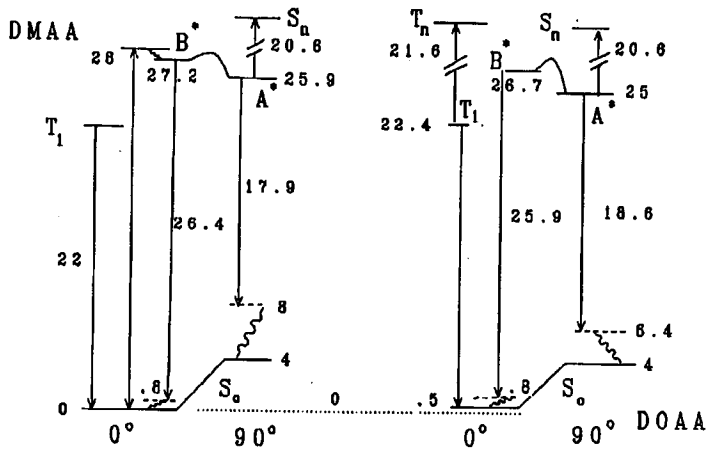
Fig. 8. Energy levels and transitions (in 10^3 cm^{-1}) of DMAA and DOAA (in ACN solution, unless otherwise stated). For DMAA the (0,0) transition in phosphorescence is measured in MTHF; the (0,0) transition in fluorescence is measured in n-propanol, $T = 77$ K [9]; the Franck–Condon relaxation in liquid ACN is equally divided into the excited and ground state contributions. The same Franck–Condon relaxation is assumed for F_b emission in DOAA. The height of the ground state potential barrier is estimated as 0.5 eV, the ground state relaxation after the F_a emission (destabilization energy) is calculated according to the previous model [24]. Setting the ground state barrier height at a lower level (as, e.g. in Ref. [30]) would not change the comparison of DOAA and DMAA, except the energy difference between the B^* and A^* states.

Marginally, it is to admit that the entropy factor, $T\Delta S_0$, is neglected in the model calculation [24]; analyzing the scarce reported data on the solubility of tetraalkylammonium salts [28] we find that the solvation entropy of the NR$^+$ ions in aprotic solvents is sometimes considerably increasing with the length of the alkyl chain. Entropy effects in different solvents, in dependence on the length of the alkyl chains, seem to be worth attention.

5.3. Inversional mode?

In their very stimulating papers [6, 7, 29] Zachariasse, Warman et al. suppose that the main factor determining the dual fluorescence ability in DMABN and in related compounds is the proximity of two close-laying $^1\pi, \pi^*$ states. In all compounds of the studied structural families which exhibit the dual fluorescence, there are, indeed, two neighbouring electronic states (or even three, as in DMAA

---

the saturated calomel electrode (SCE). As these are irreversible potentials, they strongly depend on the experimental conditions of the measurement. The effect can also be due to steric interactions of higher alkyls with the aromatic ring, resulting in non-planarity in the ground state. The effect of replacement of Me by Et was observed and discussed in the context of the TICT states of dialkylamino-pyrimidines [26]. The deviations from coplanarity (non-zero initial twist angle) should primarily influence the kinetics of the process. Now, it seems rather that the reported irreversible electrochemical oxidation potential of NEt$_3$ may be wrong, specially as the vertical ionization potential decreases at the substitution of methyls by ethyl groups [26, 27].

where the $^1n, \pi^*$ state plays an important role in less polar solvents [9]). The cited Authors [6, 7, 29] assume, however, the molecule is non-planar because of a pyramidalization of the N atom of the dialkylamino group; the inversional mode is assumed to couple the two states which results (in an unexplained way) in formation of the polar form, without mutual twisting of D and A.

Very recently, two important theoretical papers appeared, both with similar conclusions in this respect. Roos et al. [8] demonstrated that the pyramidalization of DMABN does not lead to any markedly polar structures. Very similar results are obtained by Gorse and Pesquer [30] for both, DMABN and the benzaldehyde derivative DMABA, including the solvation effects calculated for strongly polar solvents. But even a simple qualitative inspection of the symmetry rules for vibronic coupling [31] compels us to reject the concept of inversion.

In the planar DMABN (C_{2v} symmetry) the two states involved are the lowest excited $^1B_1$ and the next $^1A_1$ state. If we assume a pyramidalization of the amino nitrogen (without internal rotation), the point symmetry is reduced to C_s, with the plane of symmetry perpendicular to the aromatic ring. The symmetry of the two excited states turns to be: $A_1 \rightarrow A'$, $B_1 \rightarrow A''$. The inversional mode is symmetric in the C_s point group, a'; it cannot couple the A' and A'' states.

Thus, one can eliminate the hypothesis of the inversional coupling, not excluding a role of the proximity effects in the dynamics of the process.

5.4. The nature of the highly polar state

Summarising the results on the photophysics of DOAA, we can conclude:

(i) There is an excellent similarity between the spectra and behaviour of DOAA and DMAA or other p-carbonyl substituted dimethylanilines which have a rotable (not immobilized) $-NR_2$ group [9, 10, 21, 12].

(ii) Transient absorption spectra and the fluorescence spectra (energy of transition) give evidence that in the highly polar emitting state the separation of charges is connected with the decoupling of D^+ ($-NR_2^+$) and A^- (acetophenone radical anion) structural subunits of the molecule.

(iii) These are just the main features of the TICT state. The TICT model of the structural change is also supported by all quantum chemical calculations, e.g. [8, 9, 30].

Acknowledgments

References

[1] E. Lippert, W. Lüder, H. Boos, in: *Advances in Molecular Spectroscopy*, Ed. A. Mangini, Pergamon Press, Oxford 1962, p. 443.

[2] W. Rettig, *Topics in Current Chem.* **169**, 253 (1994).

[3] Z.R. Grabowski, K. Rotkiewicz, A. Siemiarczuk, D.J. Cowley, W. Baumann, *Nouv. J. Chim.* **3**, 443 (1979).

[4] Z.R. Grabowski, *Pure Appl. Chem.* **64**, 1249 (1992); **65**, 1751 (1993).

[5] M.C.C de Lange, D. Thorn Leeson, K.A.B. van Kuijk, A.H. Huizer, C.A.G.O. Varma, *Chem. Phys.* **174**, 425 (1993); *ibid.* **177**, 243 (1993).

[6] W. Schuddeboom, S.A. Jonker, J.M. Warman, U. Leinhos, W. Kühnle, K.A. Zachariasse, *J. Phys. Chem.* **96**, 10809 (1992).

[7] K.A. Zachariasse, T. von der Haar, A. Hebecker, U. Leinhos, W. Kühnle, *Pure Appl. Chem.* **65**, 1745 (1993).

[8] L. Serrano-Andrés, M. Merchán, B.O. Roos, R. Lindh, *J. Am. Chem. Soc.* **117**, 3189 (1995).

[9] J. Dobkowski, E. Kirkor-Kamińska, J. Koput, A. Siemiarczuk, *J. Lumin.* **27**, 339 (1982).

[10] Z.R. Grabowski, J. Dobkowski, W. Kühnle, *J. Molec. Structure* **114**, 93 (1984).

[11] T. Okada, N. Mataga, W. Baumann, *J. Phys. Chem.* **91**, 760 (1987).

[12] C. Rullière, Z.R. Grabowski, J. Dobkowski, *Chem. Phys. Lett.* **137**, 408 (1987).

[13] Z.R. Grabowski, in: *Supramolecular Photochemistry*, Ed. V. Balzani, Reidel, Dordrecht 1987, p. 319.

[14] A. Déclémy, C. Rullière, *Rev. Sci. Instrum.* **57**, 2733 (1986).

[15] J. Jasny, *J. Lumin.* **17**, 149 (1978).

[16] C. Rullière, A. Déclémy, Ph. Pée, *Rev. Phys. Appl.* **18**, 347 (1983).

[17] J. Jasny, J. Sepioł, J. Karpiuk, J. Gilewski, *Rev. Sci. Instr.* **65**, 3646 (1994).

[18] E. Kirkor-Kamińska, K. Rotkiewicz, A. Grabowska, *Chem. Phys. Lett.* **58**, 379 (1978).

[19] J. Dobkowski, J. Waluk, W. Yang, C. Rullière, W. Rettig, to be published.

[20] D.J. Cowley, I. Pasha, *J. Chem. Soc., Perkin Trans. II*, 1139 (1983).

[21] J. Dobkowski, Z.R. Grabowski, E. Heumann, D. Khechinashvili, B. Kozankiewicz, W. Kühnle, J. Sepioł, in: *Internat. Symp. on Molecular Luminescence and Photophysics – Half a Century of the Jabłoński Diagram*, Inst. of Physics, N. Copernicus Univ., Toruń 1986, p. 81.

[22] T. Shida, *Electronic Absorption Spectra of Radical Ions*, Elsevier, Amsterdam 1988, p. 275.

[23] Z.R. Grabowski, K. Rotkiewicz, W. Rubaszewska, E. Kirkor-Kamińska, *Acta Phys. Pol. A* **54**, 767 (1978).

[24] Z.R. Grabowski, J. Dobkowski, *Pure Appl. Chem.* **55**, 245 (1983).

[25] L. Meites, P. Zuman, *CRC Handbook Series in Organic Electrochemistry*, Vol. 1, CRC Publ. Co., Cleveland, (a) p. 666; (b) p. 64; (c) p. 252; (d) p. 396; (e) p. 550; (f) *ibid.* Vol. 3, p. 148.

[26] J. Herbich, Z.R. Grabowski, H. Wójtowicz, K. Golankiewicz, *J. Phys. Chem.* **93**, 3439 (1989).

[27] D.H. Aue, H.M. Webb, M.T. Bowers, *J. Am. Chem. Soc.* **98**, 311 (1976).

[28] P.T. Walden, *Z. Phys. Chem.* **55**, 698, 712 (1906).

[29] K.A. Zachariasse, Th. von der Haar, A. Hebecker, U. Leihos, W. Kühnle, in: *XVIth Internat. Conf. on Photochemistry, Abstracts*, Univ. of British Columbia, Vancouver 1993, p. 83.

[30] A.D. Gorse, M. Pesquer, *J. Phys. Chem.* **99**, 4039 (1995).

[31] R.M. Hochstrasser, C. Marzacco, *J. Chem. Phys.* **49**, 971 (1968).